Desalination and Water Treatment
www.deswater.com

doi: 10.1080/19443994.2012.677509

46 (2012) 68–74
August

Taylor & Francis
Taylor & Francis Group

The effect of condensation and evaporation pressure drop on specific heat transfer surface area and energy consumption in MED–TVC plants

R. Kouhikamali[a,*], A. Samami Kojidi[a], M. Asgari[b], F. Alamolhoda[b]

[a]*Faculty of Engineering, University of Guilan, P.O. Box 3756, Rasht, Iran*
Tel. +98 131 6690276; Fax: +98 131 6690271; email: kouhikamali@guilan.ac.ir
[b]*School of Chemical Engineering, Faculty of Engineering, University of Tehran, Tehran, Iran*

Received 26 June 2011; Accepted 6 March 2012

ABSTRACT

The aim of this article is to investigate the pressure drop of condensation inside tubes and evaporation outside tubes inside the heat exchangers of multi-effect distillation with thermal vapor compression system. The important and effective factors that have an influence on the condensation and evaporation pressure drop are investigated in this article. Also, the influence of pressure drop along the vapor flow from one effect to another on energy consumption and required heat transfer surface area is investigated. The results show that, reduction in condensation and evaporation pressure drop decreases the energy consumption up to 6.6%. In addition, with the same energy consumption, the system that has less pressure drop requires a lower specific heat transfer surface area up to 8%.

Keywords: MED–TVC; Pressure drop; Energy consumption; Specific heat transfer surface area

1. Introduction

Nowadays due to the fast growth of industrial processes, the demand for freshwater has been increasing. On the contrary, there are widespread sources of seawater or brackish water all around the world and up to now several works have been done to find out the proper methods of producing pure water from these sources. The most famous types of desalination are: multistage flash (MSF), multi-effect desalination (MED), multi-effect vapor compression, and reverse osmosis (RO). Although MSF was the most popular and the easiest route for purifying seawater in the distant past, over recent years both MED and RO have become more popular than MSF due to their significant features [1]. Some benefits of using MED like having the capability of increasing the gain output ratio (GOR) by adding extra effects, not being sensitive to the quality of the feed, and having low operating cost made it the most convenient method to desalinate water, especially in arid areas where there are sufficient sources of water such as Persian Gulf [2].

Because of the widespread use of MED among other types of desalination, it is very much imperative to investigate the effect of various parameters such as the number of effects, tube length, tube diameter, etc, which play a role in the MED's performance. The production cost and energy consumption are the two important factors that must be considered in designing a MED–TVC system. Researchers have been attempting to find ways of decreasing these costs and to optimize the process. Darwish and El-dessouky [3] compared the specific available energy, performance ratio, and specific heat transfer surface area for multi effect evaporation, MSF, and MED–TVC. It has been shown that the MED–TVC system uses less heat

*Corresponding author.

transfer surface area in comparison with two other systems for the same energy consumption. Minnich [4] reached the same conclusion by developing a simple model for the MED–TVC system operating at low top brine temperature. Al-Habshi [5] investigated the MED–TVC system by using a steady-state simulation program. The effect of thermodynamic losses on thermal performance ratio, specific heat transfer surface area, and specific flow rate of the cooling water was taken into account. Al-Habshi observed that the performance ratio depends on the motive steam condition, vapor velocity in the last effect, and the size of the steam ejector. Kamali et al. [6] investigated the influence of motive steam pressure, effect numbers, first effect steam temperature, and feed concentration in the MED–TVC system on the overall heat transfer coefficient. El-Dessouky and Ettouney [7] developed a simulation code for the MED system with shell and tube evaporators. Zhao et al. [8] performed a theoretical analysis and optimized the MED unit by comparing the GOR and specific area. They showed that, although a higher GOR could be obtained with the addition of effects, the production cost will simultaneously rise and there is an optimum point to work in. Sayyaadi and Saffari [9] optimized the process from the aspect of economics by analyzing the first and second laws of thermodynamics.

One of the most important problems in designing the MED–TVC system is the temperature difference between the evaporators. Since the fluid is in two-phase conditions, the pressure drop considerably impacts the temperature difference between the evaporators. There are three types of pressure drops in the MED: pressure drop inside the tubes, pressure drop outside the tubes, and pressure drop of steam in demisters. Each type of these pressure losses can affect the unit performance negatively from the aspects of energy consumption or production cost. Although several works have mentioned the negative effect of pressure drop [10,11], a comprehensive research into these kinds of pressure drops separately and comparing the amount of their effect has not been done yet.

In the present work, we developed a simulation code to model the behavior of unit accurately. At first, we compared two of the most convenient correlations of pressure drop calculations to show that they resulted in nearly the same responses. Next, we applied the Friedel correlation to calculate the pressure drop in each section for different cases to realize the parameters that could influence the energy consumption or construction cost. At last, we compared and analyzed the calculated data for all the cases to investigate the effect of different parameters on pressure drop and performance of each case.

2. Process description

The scheme of a MED–TVC unit is illustrated in Fig. 1. The main parts of a MED–TVC unit are shell and tube evaporators, a condenser, and a thermo compressor. The motive steam that is generated in the boiler enters the thermo compressor and sucks some of the vapor that is generated in the last effect and then the mixed vapor gets compressed. This compressed vapor passes through the tubes of the first effect, while the preheated seawater falls over the outside surface of the tubes and evaporation takes place. The generated steam is passed through demisters and enters the next effect. This process goes on until the last effect. The steam is divided into two parts; the first part is sucked into the thermo compressor and the second part is directed to the condenser.

3. Two-phase flow pressure drop

Different correlations were proposed to calculate the two-phase flow pressure drop. Two of them, which well prove the experimental data, are used in this article [12,13].

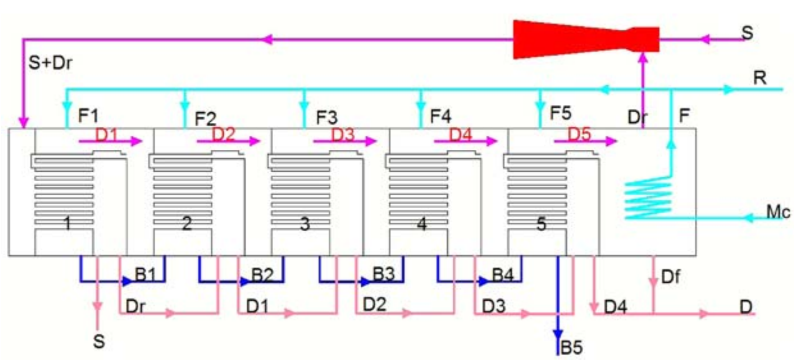

Fig. 1. A MED–TVC unit configuration.

3.1. Friedel correlation

This method utilizes a two-phase multiplier according to Eq. (1) [12]:

$$\Delta p_{\text{frict}} = \Delta p_{\text{L}} \varphi^2_{\text{Lo}} \tag{1}$$

Δp_{L} is the pressure drop of the fluid, which is considered as the liquid phase.

$$\Delta p_{\text{L}} = 4 f_{\text{L}} \left(\frac{\text{L}}{d_i}\right) \dot{m}^2_{\text{total}} (1-X)^2 \left(\frac{1}{2p_{\text{L}}}\right) \tag{2}$$

The liquid friction factor and liquid Reynolds number are obtained from Eqs. (3) and (4):

$$f = \frac{0.079}{\text{Re}^{0.25}} \tag{3}$$

$$\text{Re} = \frac{\dot{m}_{\text{total}} d_i}{\mu} \tag{4}$$

A two-phase multiplier is shown in Eq. (5).

$$\varphi^2_{\text{Lo}} = E + \frac{3.24 F H}{\text{Fr}_h^{0.045} \text{We}_{\text{L}}^{0.035}} \tag{5}$$

Fr_h, E, F, and H are as follows:

$$\text{Fr}_h = \frac{\dot{m}^2_{\text{total}}}{g d_i \rho_h^2} \tag{6}$$

$$E = (1-X)^2 + X^2 \frac{\rho_{\text{L}} f_{\text{G}}}{\rho_{\text{G}} f_{\text{L}}} \tag{7}$$

$$F = X^{0.78} (1-X)^{0.224} \tag{8}$$

$$H = \left(\frac{\rho_{\text{L}}}{\rho_{\text{G}}}\right)^{0.91} \left(\frac{\mu_{\text{G}}}{\mu_{\text{L}}}\right)^{0.19} \left(1 - \frac{\mu_{\text{G}}}{\mu_{\text{L}}}\right)^{0.7} \tag{9}$$

The liquid Weber number We_{L} is defined in Eq. (10):

$$\text{We}_{\text{L}} = \frac{\dot{m}^2_{\text{total}} d_i}{\sigma \rho_h} \tag{10}$$

And the homogeneous density (ρ_h) is:

$$\rho_h = \left(\frac{X}{\rho_{\text{G}}} + \frac{1-X}{\rho_{\text{L}}}\right)^{-1} \tag{11}$$

Friedel's method is typically recommended when the ratio of μ_{L} to μ_{G} is < 1,000.

3.2. Lockhart–Martinelli correlation [13]

This method gives the two-phase frictional pressure drop based on a two-phase multiplier for the liquid-phase or vapor-phase, respectively, as follows:

$$\Delta p_{\text{frict}} = \varphi^2_{\text{Ltt}} \Delta p_{\text{L}} \tag{12}$$

$$\Delta p_{\text{frict}} = \varphi^2_{\text{Gtt}} \Delta p_{\text{G}} \tag{13}$$

Δp_{L} is obtained from Eq. (2) and Δp_{G} can be calculated from Eq. (14).

$$\Delta p_{\text{G}} = 4 f_{\text{G}} \left(\frac{L}{d_i}\right) \dot{m}^2_{\text{total}} X^2 \left(\frac{1}{2\rho_{\text{G}}}\right) \tag{14}$$

The single-phase friction factors of the liquid and vapor (f_{L} and f_{G}), are calculated by Eq. (3) with their respective physical properties. The corresponding two-phase multipliers are obtained from Eqs. (15) and (16).

$$\varphi^2_{\text{Ltt}} = 1 + \frac{C}{X_{\text{tt}}} + \frac{1}{X^2_{\text{tt}}}, \ \textit{for}\ \text{Re}_{\text{L}} > 4,000 \tag{15}$$

$$\varphi^2_{\text{Gtt}} = 1 + C X_{\text{tt}} + X^2_{\text{tt}}, \ \text{for}\ \text{Re}_{\text{L}} < 4,000 \tag{16}$$

X_{tt} is the Martinelli parameter for both phases in the turbulent regime that is shown in Eq. (17).

$$X_{\text{tt}} = \left(\frac{1-X}{X}\right)^{0.9} \left(\frac{\rho_{\text{G}}}{\rho_{\text{L}}}\right)^{0.5} \left(\frac{\mu_{\text{L}}}{\mu_{\text{G}}}\right)^{0.1} \tag{17}$$

The value of C in Eqs. (15) and (16) depends on the regimes of the liquid and vapor phases. In the considered cases in the present database, both phases are in the turbulent regime and for this condition, C should be assumed to be 20 [13].

4. Case study

We investigated the effect of pressure drop in four real MED–TVC units. A simulation program has been prepared to obtain the specific heat transfer surface area and GOR for each unit in different conditions. Table 1 depicts the characteristics of these MED–TVC units.

Because of the presence of a two-phase flow in the tube side, shell side, and saturated vapor flow across the demister in MED plants, any pressure drop results in decreasing the temperature of the flowing vapor. The vapor generating in an effect is the heating media in the next effect. Therefore, it is evident that these temperature drops cause less temperature difference between condensing vapor and boiling seawater in a MED plant. As the surface area of MED plants like all other thermal plants is calculated by considering the temperature difference, loss of temperature difference absolutely leads to surface area ascending. Otherwise, in order to keep the surface area of the MED plants constant by the rising pressure drop, the temperature of the first effect should be raised in such a way that the total effective temperature difference (LMTD) in the plant remains constant. In MED–TVC plants, the increasing temperature of the first effect is equal to raising the discharge pressure of the thermo compressor. It is obvious that in constant motive steam pressure, the steam consumption increases as the discharge pressure of the thermo compressor rises. So, the loss of pressure in a two-phase flow in MED plants leads to an increase in the surface area or a decrease in the GOR (increase in steam consumption).

The pressure drop of condensation inside the tubes, evaporation in the shell side, and also vapor pressure drop at the demister surface are calculated by using correlations described earlier in Section 3. The specific heat transfer surface area and GOR have been considered to evaluate the influence of pressure drop inside and outside the tubes on the performance of the system.

Table 1
Different investigated cases of MED–TVC units

Parameter	Unit	Quantity
Case 1		
Total product	MIGD	1
Number of effects		5
TBT	℃	64
Tube length	m	4.6
Tube ID	mm	28.575
Tube thickness	mm	0.7
Case 2		
Total product	MIGD	1
Number of effects		4
TBT	℃	64
Tube length	m	4.6
Tube ID	mm	28.575
Tube thickness	mm	0.7
Case 3		
Total product	MIGD	1.5
Number of effects		5
TBT	℃	64
Tube length	m	7.2
Tube ID	mm	28.575
Tube thickness	mm	0.7
Case 4		
Total product	MIGD	1.5
Number of effects		5
TBT	℃	64
Tube length	m	4.6
Tube ID	mm	28.575
Tube thickness	mm	0.7

5. Results and discussion

The comparison between Friedel and Lockhart–Martinelli correlations for pressure drop is given in Fig. 2 showing the required specific heat transfer surface area for all four units. As it is evident from Fig. 2, the specific heat transfer areas obtained from each of the two correlations are nearly the same. Therefore, every equation could result in an accurate response. Due to the widespread use of the Friedel correlation for estimating the pressure drop in MED systems, this correlation has been used to calculate the pressure drop of each part [14,15].

Another point that should be mentioned is that the specific heat transfer areas for all four units are different from each other. These differences are due to differences in the geometry and capacity of systems that can noticeably influence the pressure drop and the heat transfer coefficient in these systems, which causes different specific heat transfer areas [11].

Fig. 3 shows the effect of vapor pressure drop at the demister surface on specific heat transfer surface area. Pressure drop that takes place by the flowing vapor along the demister surface increases the specific heat transfer surface area up to 2%.

The demister area in Case 1 is considered twice the others in order to realize the parameters that affect the pressure drop across the demister. So, it could be conspicuously seen that Case 1 had greatest pressure drop among all the cases.

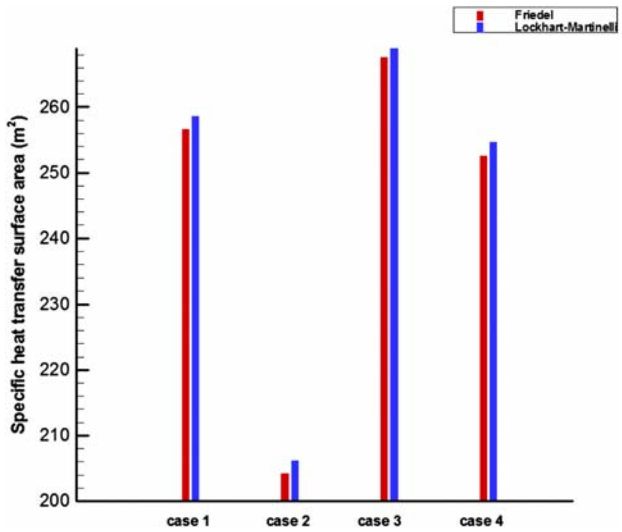

Fig. 2. The comparison between Friedel and Lockhart–Martinelli correlations.

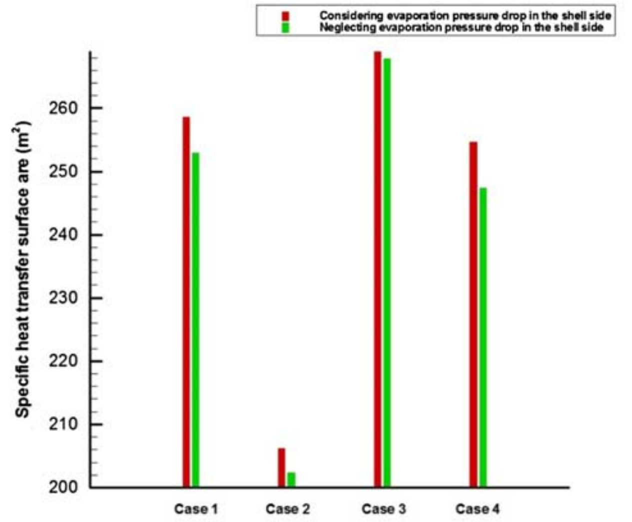

Fig. 4. The effect of evaporation pressure drop in the shell side on the specific heat transfer surface area.

Fig. 4 compares the specific heat transfer surface area for each unit by both neglecting and considering the evaporation pressure drop in the shell side. This pressure drop increases the specific heat transfer surface area up to 3%. Comparing the shell side pressure drop of all cases, it is obvious that the specific heat transfer area of Case 4 increases more than others. This is because of two main reasons. The first reason is that as the product rates in Cases 3 and 4 are more than in Cases 1 and 2, the amount of seawater feed that enters the shell side of each effect is larger.

Another reason is that because of the smaller length of tubes in Case 4 than Case 3 the cross-sectional area for the passing seawater and vapor in the shell side is considerably smaller than Case 3 in which the tube length is larger. These two reasons are causes for the greater turbulency in the shell side and larger friction factor, which result in an increasing pressure drop.

The influence of condensation pressure drop inside the tubes on specific heat transfer surface area is shown in Fig. 5. As can be seen, the pressure drop inside the tubes increases the specific heat transfer surface area. The greatest pressure drop is related to Case 3, which rises the specific heat transfer area by about 7%. As the condensation pressure drop inside the tube is a linear function of tube length, it is expected that Case 3 has a

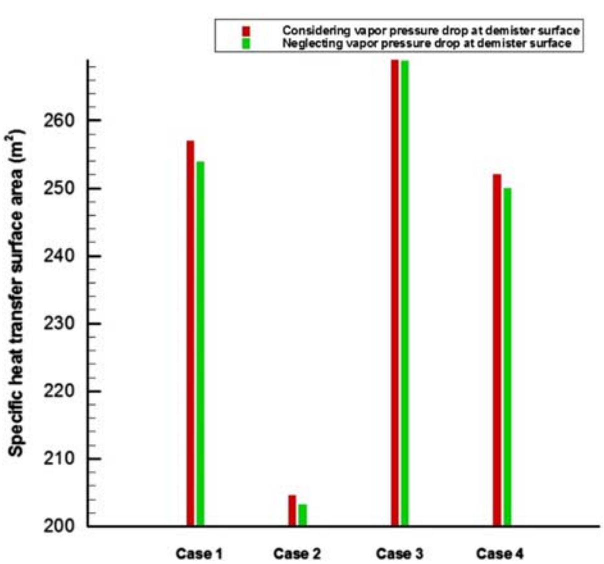

Fig. 3. The effect of vapor pressure drop at demister surface on the specific heat transfer surface area.

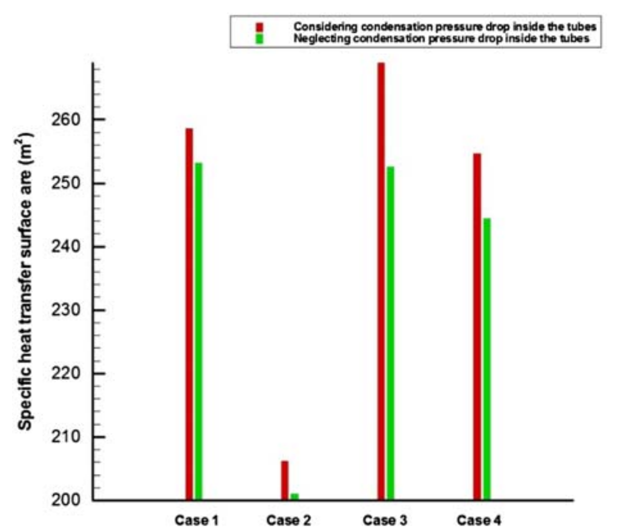

Fig. 5. The effect of condensation pressure drop inside the tubes on the specific heat transfer surface area.

greater pressure drop inside the tube because of condensation. In addition, since the vapor velocity and friction factor inside tubes are directly related to the production rate, a higher production rate can lead to a higher pressure drop.

Fig. 6 shows the specific heat transfer surface area via-a-vis the total pressure drop in comparison with neglecting the total pressure drop. Owing to the latter, the specific heat transfer surface area gets considerably reduced than in the case when the total pressure drop is considered. It is shown that the total pressure drop in MED–TVC units increases the specific heat transfer surface area up to 8%, with the greatest effect belonging to Case 3. As the pressure drop portion inside the tubes is higher than other kinds of pressure drops, the total pressure drop increases heat transfer surface area of Case 3 more than the others.

Fig. 7 shows the comparison between different kinds of pressure drops for all four cases. The comparison between four cases shows that the variation in pressure drops has no similar trend in those cases. The parameter that has the most effect on pressure drop for each of four cases is different.

Noticing Case 1, it could be realized that the demister pressure drop is a key parameter in the total pressure drop because the surface area of a demister is overdesigned, which results in a higher pressure drop.

For Case 3 where the friction factor and length of tubes are higher than others, the pressure drop due to condensation of vapor inside the tubes plays a key role is estimating the total pressure drop. In this case, it can be really seen that because of the significant influence of pressure drop inside the tubes, the total pressure drop is higher than others.

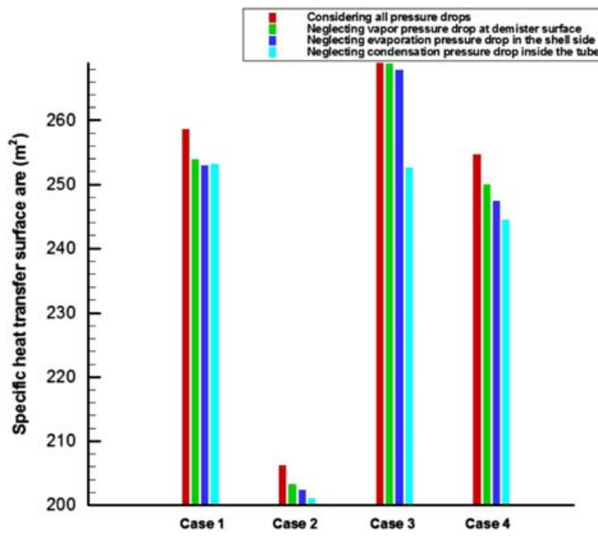

Fig. 7. The comparison between the effect of different types of pressure drop on the specific heat transfer surface area.

Going to Case 4, it is evident that both shell side and demister surface pressure drop have large portions in total pressure drop, which is due to high vapor velocity in the shell side of Case 4.

Comparing the different kinds of pressure drops for Case 2 shows that each kind of pressure drop affects the unit performance as much as others do and none of them increase the heat transfer area of this case severely. Because of this fact, we can easily see that for this case the total pressure drops influence on the unit performance is smaller than others.

The influence of the total pressure drop on energy consumption is shown in Fig. 8. As can be seen, the pressure drop increases the energy consumption while

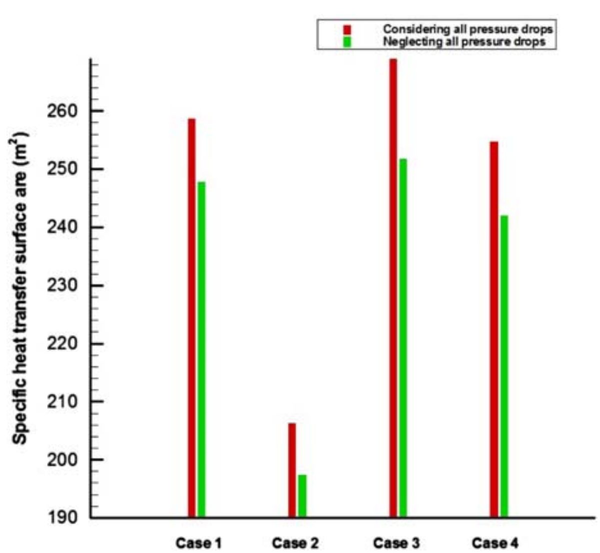

Fig. 6. The effect of the total pressure drop on the specific heat transfer surface area.

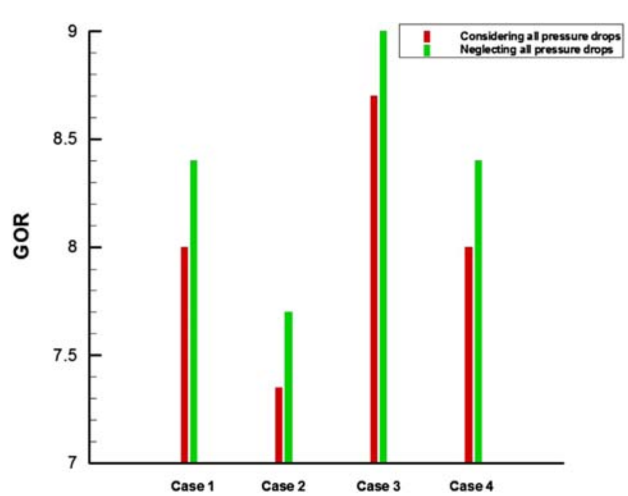

Fig. 8. The effect of the total pressure drop on energy consumption.

this negative effect is greater for cases in which the total product is smaller. The greatest effect on the energy consumption belongs to Case 1 in which the total pressure drop increases energy consumption of this unit up to 6.6%.

6. Conclusion

Now, it is obvious that increasing pressure losses can lead to higher energy consumption and construction cost. So, optimizing process in the sense of pressure drop can result in better performance of the unit. As it is shown in the last section, there are several parameters that can affect the pressure drop. Increasing pressure drop in each section elevates total pressure drop. So, it is very much imperative to design a unit in which all kinds of pressure drops in different sections are low and nearly the same. Among different kinds of pressure losses, it seems that condensation pressure drop inside the tubes has the most influence on increasing the specific heat transfer surface area. Because of this fact, the rising pressure drop in the tube side, which can negatively influence the unit performance should be particularly noticed. However to avoid the negative effect of pressure drop on unit performance, tube length, tube diameter, shell diameter, and number of tubes should be designed in such a way that the total pressure drop reaches its minimum.

Nomenclature

B	—	flow rate of brine blow down, m^3/h
D	—	flow rate of distillate water, m^3/h
D_f	—	flow rate of distillate water produced in a condenser, m^3/h
D_r	—	flow rate of entrained steam, m^3/h
d_i	—	tubes internal diameter, m
E	—	Friedel parameter in two-phase multiplier
F	—	feed flow rate in the effects, m^3/h
F	—	Friedel parameter
f	—	Friction factor
g	—	acceleration due to gravity, m/s^2
H	—	Friedel factor
L	—	tube length, m
M_c	—	total flow rate of seawater, m^3/h
m_{total}	—	total fluid mass flow rate
Δp_{frict}	—	two-phase fractional pressure drop, Pa
Δp_G	—	vapor-phase pressure drop, Pa
Δp_L	—	liquid-phase pressure drop, Pa
R	—	flow rate of rejected water, m^3/h
S	—	flow rate of motive steam, m^3/h
TBT	—	top brine temperature, ℃
X	—	vapor quality

Greek symbols

φ_{Lo}	—	liquid-phase multiplier
φ_{Go}	—	vapor-phase multiplier
φ_{Ltt}	—	two-phase multiplier of Martinelli relative to liquid
φ_{Gtt}	—	two-phase multiplier of Martinelli relative to vapor
μ	—	dynamic viscosity, Ns/m^2
σ	—	surface tension

Dimensionless numbers

Fr	—	Froude number
Re	—	Reynolds number
We	—	Weber number

References

[1] M. Al-Shammiri, M. Safar, Multi-effect distillation plants: State of the art, Desalination 126 (1999) 45–59.

[2] R.K. Kamali, S. Mohebinia, Experience of design and optimization of multi-effects desalination systems in Iran, Desalination 222 (2008) 639–645.

[3] M.A. Darwish, H.T. El-Dessouky, The heat recovery thermal vapor-compression desalting system: A comparison with other thermal desalination processes, Appl. Thermal Eng. 18 (1996) 523–537.

[4] K. Minnich, J. Tonner, F. Neu, A comparison of heat transfer requirement and evaporator cost for MED–TVC and MSF, Proc. IDA World Cong. Desalin. Water Sci., Abu Dhabi, UAE 3 (1995) 233–257.

[5] S.O. Al-Habshi, Simulation and economic study of the MED–TVC units at Umm Al-Nar desalination plant, Thesis, UAE, 2002.

[6] R.K. Kamali, A. Abbassi, S.A. Sadough Vanini, M. Saffar Avval, Thermodynamic design and parametric study of MED–TVC, Desalination 222 (2008) 596–604.

[7] H.M. Ettouney, H. El-Dessouky, A simulator for thermal desalination process, Desalination 125 (1999) 277–291.

[8] D. Zhao, J. Xuea, S. Lia, H. Suna, Q. Zhang, Theoretical analyses of thermal and economical aspects of multi-effect distillation desalination dealing with high-salinity wastewater, Desalination 273 (2011) 292–298.

[9] H. Sayyaadi, A. Saffari, Thermoeconomic optimization of multi-effect distillation desalination systems, Appl. Energy 87 (2010) 1122–1133.

[10] H. Choi, T. Lee, Y. Kim, S. Song, Performance improvement of multi effect distiller with thermal vapor compression system by exergy analysis, Desalination 182 (2005) 239–249.

[11] N. Pourkhiabani, M. Alishiri, R. Kouhikamali, Pressure drop and heat transfer analysis in multi effect desalination units, IDA World Congress—Atlantis, The Palm—Dubai, UAE, November 7–12, 2009.

[12] L. Friedel, Improved friction pressure drop correlations for horizontal and vertical two-phase pipe flow, European Two-Phase Flow Group Meeting, Paper E2, Ispra, Italy, June 1979.

[13] R.W. Lockhart, R.C. Martinelli, Proposed correlation of data for isothermal two-phase tow-component flow in pipes, Chem. Eng. Progr. 45 (1949) 39–45.

[14] H. El-Dessouky, I. Alatiqi, S. Bingulac, H. Ettouney, Steady-state analysis of the multiple effect evaporation desalination process, Chem. Eng. Technol. 21 (1998) 5.

[15] T.W. Lim, J.H. Kim, An experimental investigation of pressure drop in flow boiling of pure refrigerants and their mixture in horizontal tube, JSME Int. J. B 48 (2005) 92–98.